McGraw-Hill Series in Mechanical Engineering

Jack P. Holman, *Southern Methodist University*
Consulting Editor

Anderson: *Modern Compressible Flow: With Historical Perspective*
Barron: *Cryogenic Systems*
Eckert: *Introduction to Heat and Mass Transfer*
Eckert and Drake: *Analysis of Heat and Mass Transfer*
Eckert and Drake: *Heat and Mass Transfer*
Ham, Crane, and Rogers: *Mechanics of Machinery*
Hartenberg and Denavit: *Kinematic Synthesis of Linkages*
Hinze: *Turbulence*
Hutton: *Applied Mechanical Vibrations*
Jacobsen and Ayre: *Engineering Vibrations*
Juvinall: *Engineering Considerations of Stress, Strain, and Strength*
Kays and Crawford: *Convective Heat and Mass Transfer*
Lichty: *Combustion Engine Processes*
Martin: *Kinematics and Dynamics of Machines*
Phelan: *Dynamics of Machinery*
Phelan: *Fundamentals of Mechanical Design*
Pierce: *Acoustics: An Introduction to Its Physical Principles and Applications*
Raven: *Automatic Control Engineering*
Schenk: *Theories of Engineering Experimentation*
Schlichting: *Boundary-Layer Theory*
Shigley: *Dynamic Analysis of Machines*
Shigley: *Kinematic Analysis of Mechanics*
Shigley: *Mechanical Engineering Design*
Shigley: *Simulation of Mechanical Systems*
Shigley and Uicker: *Theory of Machines and Mechanisms*
Stoecker: *Refrigeration and Air Conditioning*

MODERN COMPRESSIBLE FLOW

With Historical Perspective

John D. Anderson, Jr.

Professor of Aerospace Engineering
University of Maryland, College Park

McGraw-Hill Book Company

New York St. Louis San Francisco Auckland Bogotá Hamburg
Johannesburg London Madrid Mexico Montreal New Delhi
Panama Paris São Paulo Singapore Sydney Tokyo Toronto

11.7 SUPERSONIC NOZZLE DESIGN

In order to expand an internal steady flow through a duct from subsonic to supersonic speed, we established in Chap. 5 that the duct has to be convergent-divergent in shape, as sketched in Fig. 11.11*a*. Moreover, we developed relations for the local Mach number, and hence the pressure, density, and temperature, as functions of local area ratio A/A^*. However, these relations assumed quasi-one-dimensional flow, whereas, strictly speaking, the flow in Fig. 11.11*a* is two-dimensional. Moreover, the quasi-one-dimensional theory tells us nothing about the proper *contour* of the duct, i.e., what is the proper variation of area with respect to the flow direction $A = A(x)$. If the nozzle contour is not proper, shock waves may occur inside the duct.

The method of characteristics provides a technique for properly designing the contour of a supersonic nozzle for shockfree, isentropic flow, taking into account the multidimensional flow inside the duct. The purpose of this section is to illustrate such an application.

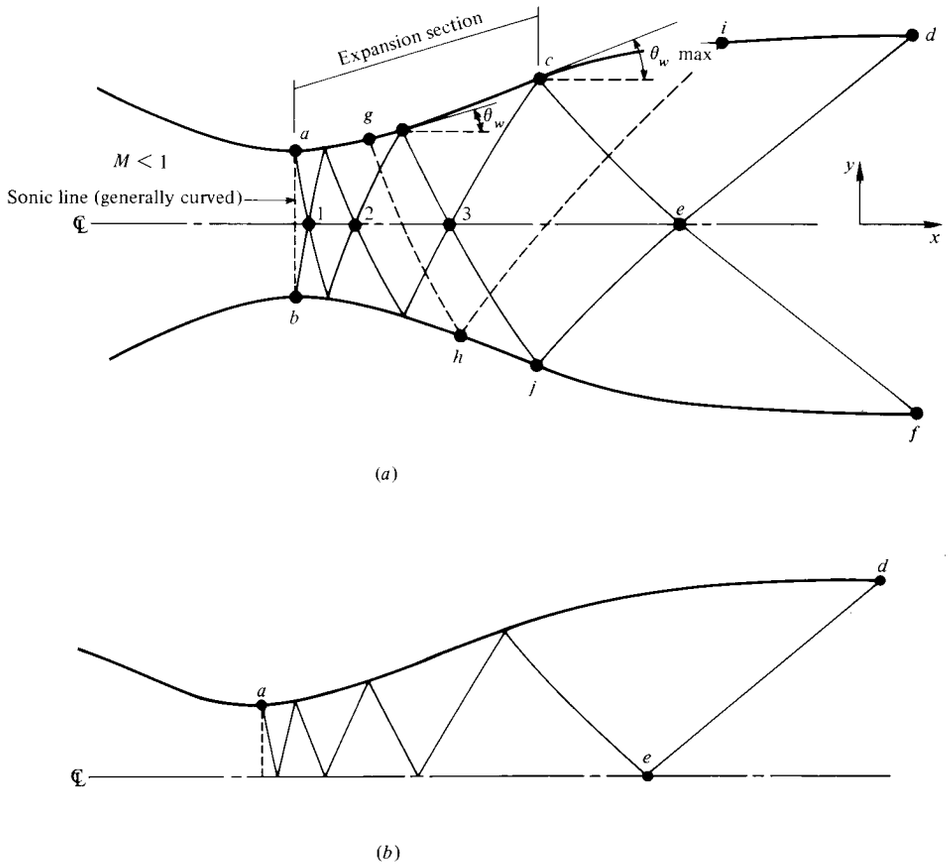

Figure 11.11 Schematic of supersonic nozzle design by the method of characteristics.

The subsonic flow in the convergent portion of the duct in Fig. 11.11*a* is accelerated to sonic speed in the throat region. In general, because of the multidimensionality of the converging subsonic flow, the sonic line is gently curved. However, for most applications, we can assume the sonic line to be straight, as illustrated by the straight dashed line from *a* to *b* in Fig. 11.11*a*. Downstream of the sonic line, the duct diverges. Let θ_w represent the angle of the duct wall with respect to the x direction. The section of the nozzle where θ_w is increasing is called the *expansion* section; here, expansion waves are generated and propagate across the flow downstream, reflecting from the opposite wall. Point *c* is an inflection point of the contour, where $\theta_w = \theta_{w_{max}}$. Downstream of point *c*, θ_w decreases until the wall becomes parallel to the x direction at points *d* and *f*. The section from *c* to *d* is a "straightening" section specifically designed to cancel all the expansion waves generated by the expansion section. For example, as shown by the dashed line in Fig. 11.11*a*, the expansion wave generated at *g* and reflected at *h* is cancelled at *i*. Also shown in Fig. 11.11*a* are the characteristic lines going through points *d* and *f* at the nozzle exit. These characteristics represent infinitesimal expansion waves in the nozzle, i.e., Mach waves. Tracing these two characteristics upstream, we observe multiple reflections up to the throat region. The area *acejb* is the expansion region of the nozzle, covered with both left- and right-running characteristics. Such a region with waves of both families is defined as a *nonsimple region* (analogous to the nonsimple waves described for unsteady one-dimensional flow in Sec. 7.7). In this region, the characteristics are curved lines. In contrast, the regions *cde* and *jef* are covered by waves of only one family because the other family is cancelled at the wall. Hence, these are *simple regions*, where the characteristic lines are straight. Downstream of *def*, the flow is uniform and parallel, at the desired Mach number. Finally, due to the symmetry of the nozzle flow, the waves (characteristics) generated from the top wall act as if they are "reflected" from the centerline. This geometric ploy due to symmetry allows us to consider in our calculations only the flow above the centerline, as sketched in Fig. 11.11*b*.

Supersonic nozzles with gently curved expansion sections as sketched in Fig. 11.11*a* and *b* are characteristic of wind tunnel nozzles where high-quality, uniform flow is desired in the test section (downstream of *def*). Hence, wind tunnel nozzles are long, with a relatively slow expansion. By comparison, rocket nozzles are short in order to minimize weight. Also, in cases where rapid expansions are desirable, such as the nonequilibrium flow in modern gasdynamic lasers (see Ref. 21), the nozzle length is as short as possible. In such *minimum-length nozzles*, the expansion section in Fig. 11.11*a* is shrunk to a point, and the expansion takes place through a centered Prandtl-Meyer wave emanating from a sharp-corner throat with an angle $\theta_{w_{max,\,ML}}$, as sketched in Fig. 11.12*a*. The length of the supersonic nozzle, denoted as L in Fig. 11.12*a* is the minimum value consistent with shockfree, isentropic flow. If the contour is made shorter than L, shocks will develop inside the nozzle.

Assume that the nozzles sketched in Figs. 11.11*a* and 11.12*a* are designed for the same exit Mach numbers. For the nozzle in Fig. 11.11*a* with an arbitrary

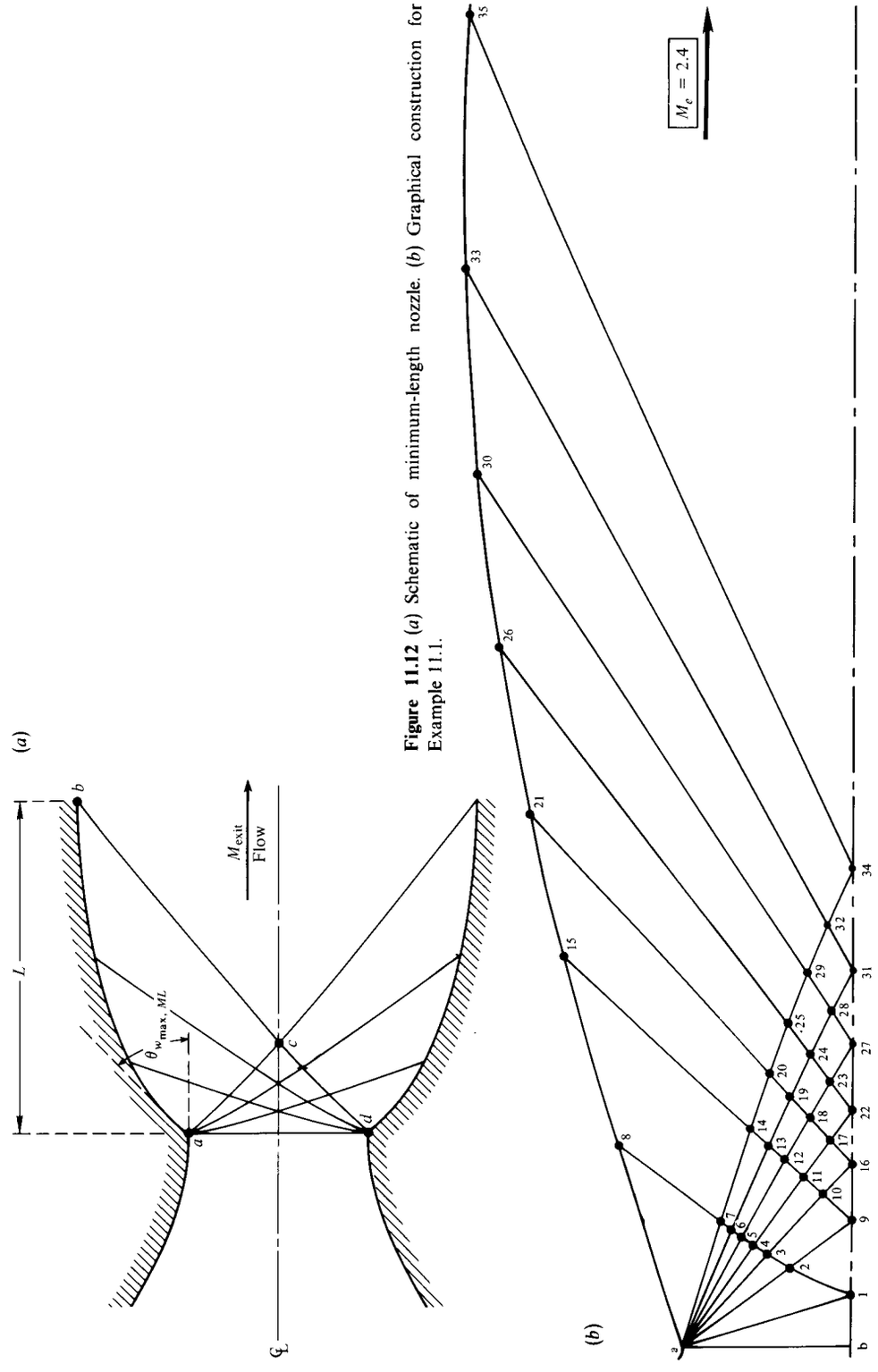

Figure 11.12 (*a*) Schematic of minimum-length nozzle. (*b*) Graphical construction for Example 11.1.

expansion contour *ac*, multiple reflections of the characteristics (expansion waves) occur from the wall along *ac*. A fluid element moving along a streamline is constantly accelerated while passing through these multiple reflected waves. In contrast, for the minimum-length nozzle shown in Fig. 11.12*a*, the expansion contour is replaced by a sharp corner at point *a*. There are no multiple reflections, and a fluid element encounters only two systems of waves—the right-running waves emanating from point *a* and the left-running waves emanating from point *d*. As a result, $\theta_{w_{max,\,M_L}}$ in Fig. 11.12*a* must be larger than $\theta_{w_{max}}$ in Fig. 11.11*a*, although the exit Mach numbers are the same.

Let ν_M be the Prandtl-Meyer function associated with the design exit Mach number. Hence, along the C_+ characteristic *cb* in Fig. 11.12*a*, $\nu = \nu_M = \nu_c = \nu_b$. Now consider the C_- characteristic through points *a* and *c*. At point *c*, from Eq. (11.20),

$$\theta_c + \nu_c = (K_-)_c \tag{11.28}$$

However, $\theta_c = 0$ and $\nu_c = \nu_M$. Hence, from Eq. (11.28),

$$(K_-)_c = \nu_M \tag{11.29}$$

At point *a*, along the same C_- characteristic *ac*, from Eq. (11.20),

$$\theta_{w_{max,\,M_L}} + \nu_a = (K_-)_a \tag{11.30}$$

Since the expansion at point *a* is a Prandtl-Meyer expansion from initially sonic conditions, we know from Sec. 4.13 that $\nu_a = \theta_{w_{max,\,M_L}}$. Hence, Eq. (11.30) becomes

$$\theta_{w_{max,\,M_L}} = \tfrac{1}{2}(K_-)_a \tag{11.31}$$

However, along the same C_- characteristic, $(K_-)_a = (K_-)_c$; hence Eq. (11.31) becomes

$$\theta_{w_{max,\,M_L}} = \tfrac{1}{2}(K_-)_c \tag{11.32}$$

Combining Eqs. (11.29) and (11.32), we have

$$\boxed{\theta_{w_{max,\,M_L}} = \frac{\nu_M}{2}} \tag{11.33}$$

Equation (11.33) demonstrates that, *for a minimum-length nozzle the expansion angle of the wall downstream of the throat is equal to one-half the Prandtl-Meyer function for the design exit Mach number*. For other nozzles such as that sketched in Fig. 11.11*a*, the maximum expansion angle is *less* than $\nu_M/2$.

The shape of the finite-length expansion section in Fig. 11.11*a* can be somewhat arbitrary (within reason). It is frequently taken to be a circular arc with a diameter larger than the nozzle throat height. However, once the shape of the expansion section is chosen, then its length and $\theta_{w_{max}}$ are determined by the design exit Mach number. These properties can be easily found by noting that the characteristic line from the end of the expansion section intersects the centerline at point *e*, where the local Mach number is the same as the design exit Mach number. Hence, to find the expansion section length and $\theta_{w_{max}}$, simply keep track of the centerline Mach number (at points 1, 2, 3, etc.) as you construct your characteristics solution starting from the throat region. When the centerline Mach number equals the design exit Mach number, this is point *e*. Then

Table 11.1

Point No.	$K_- = \theta + \nu$	$K_+ = \theta - \nu$	$\theta = \frac{1}{2}(K_- + K_+)$	$\nu = \frac{1}{2}(K_- - K_+)$	M	μ	Comments
1	0.75	0	0.375†	0.375†	1.04	74.1	
2	6.75	0	3.375†	3.375†	1.19	57.2	
3	12.75	0	6.375†	6.375†	1.31	49.8	
4	18.75	0	9.375†	9.375†	1.41	45.2	
5	24.75	0	12.375†	12.375†	1.52	41.1	
6	30.75	0	15.375†	15.375†	1.62	38.1	
7	36.75	0	18.375†	18.375†	1.72	35.6	
8	36.75†	0†			1.72†	35.6†	Same as point 7
9	6.75†	−6.75	0†	6.75	1.32	49.3	
10	12.75†	−6.75†	3	9.75	1.43	44.4	
11	18.75†	−6.75†	6	12.75	1.53	40.8	
12	24.75†	−6.75†	9	15.75	1.63	37.8	
13	30.75†	−6.75†	12	18.75	1.73	35.3	
14	36.75†	−6.75†	15	21.75	1.84	32.9	
15	36.75†	−6.75†	15†	21.75†	1.84†	32.9†	Same as point 14
16	12.75†	−12.75	0†	12.75	1.53	40.8	
17	18.75†	−12.75†	3	15.75	1.63	37.8	
18	24.75†	−12.75†	6	18.75	1.73	35.3	
19	30.75†	−12.75†	9	21.75	1.84	32.9	
20	36.75†	−12.75†	12	24.75	1.94	31.0	
21	36.75†	−12.75†	12†	24.75†	1.94†	31.0†	Same as point 20
22	18.75†	−18.75	0†	18.75	1.73	35.3	
23	24.75†	−18.75†	3	21.75	1.84	32.9	
24	30.75†	−18.75†	6	24.75	1.94	31.0	
25	36.75†	−18.75†	9	27.75	2.05	29.2	
26	36.75†	−18.75†	9†	27.75†	2.05†	29.2†	Same as point 25
27	24.75†	−24.75	0†	24.75	1.94	31.0	
28	30.75†	−24.75†	3	27.75	2.05	29.2	
29	36.75†	−24.75†	6	30.75	2.16	27.6	
30	36.75†	−24.75†	6†	30.75†	2.16†	27.6†	Same as point 29
31	30.75†	−30.75	0†	30.75	2.16	27.6	
32	36.75†	−30.75	3	33.75	2.28	26.0	
33	37.75†	−30.75†	3†	33.75†	2.28†	26.0†	Same as point 32
34	36.75†	−36.75	0†	36.75	2.4	24.6	
35	36.75†	−36.75†	0†	36.75†	2.4†	24.6†	Same as point 34

† Known quantities at beginning of each step.

the expansion section is terminated at point c, which fixes both its length and the value of $\theta_{w_{max}}$.

Example 11.1 Compute and graph the contour of a two-dimensional minimum-length nozzle for the expansion of air to a design exit Mach number of 2.4.

SOLUTION The results of this problem are given in Fig. 11.12*b*. To begin with, the sonic line at the throat, *ab*, is assumed to be straight. The first characteristic $(a - 1)$ emanating from the sharp throat is chosen as inclined only slightly from the normal sonic line. ($\Delta\theta = 0.375°$; hence $\theta + \nu = 0.75°$ and $dy/dx = \theta - \mu = -73.725°$.) The remainder of the expansion fan is divided into six increments with $\Delta\theta = 3°$. The total corner angle $\theta_{w_{max}} = \nu/2 = 36.75°/2 = 18.375°$. The values of K_+, K_-, θ, and ν are tabulated in Table 11.1 for all grid points. The nozzle contour is drawn by starting at the throat corner (where $\theta_a = \theta_{w_{max}} = 18.375°$), drawing a straight line with an average slope, $\frac{1}{2}(\theta_a + \theta_8)$, and defining point 8 on the contour as the intersection of this straight line with the left-running characteristic 7–8. Point 15 is located by the intersection of a straight line through point 8 having a slope of $\frac{1}{2}(\theta_8 + \theta_{15})$ with the left-running characteristic 14–15. This process is repeated to generate the remainder of the contour, points 21, 26, etc.

For this example, the computed area ratio $A_e/A^* = 2.33$. This is within 3 percent of the value $A_e/A^* = 2.403$ from Table A.1. This small error is induced by the graphical construction of Fig. 11.12*b*, and by the fact that only seven increments are chosen for the corner expansion fan. For a more accurate calculation, finer increments should be used, resulting in a more closely spaced characteristic net throughout the nozzle.

APPENDIX

Table A.1 Isentropic flow properties

M	$\frac{p_o}{p}$	$\frac{\rho_o}{\rho}$	$\frac{T_o}{T}$	$\frac{A}{A^*}$
0.2000−01	0.1000+01	0.1000+01	0.1000+01	0.2894+02
0.4000−01	0.1001+01	0.1001+01	0.1000+01	0.1448+02
0.6000−01	0.1003+01	0.1002+01	0.1001+01	0.9666+01
0.8000−01	0.1004+01	0.1003+01	0.1001+01	0.7262+01
0.1000+00	0.1007+01	0.1005+01	0.1002+01	0.5822+01
0.1200+00	0.1010+01	0.1007+01	0.1003+01	0.4864+01
0.1400+00	0.1014+01	0.1010+01	0.1004+01	0.4182+01
0.1600+00	0.1018+01	0.1013+01	0.1005+01	0.3673+01
0.1800+00	0.1023+01	0.1016+01	0.1006+01	0.3278+01
0.2000+00	0.1028+01	0.1020+01	0.1008+01	0.2964+01
0.2200+00	0.1034+01	0.1024+01	0.1010+01	0.2708+01
0.2400+00	0.1041+01	0.1029+01	0.1012+01	0.2496+01
0.2600+00	0.1048+01	0.1034+01	0.1014+01	0.2317+01
0.2800+00	0.1056+01	0.1040+01	0.1016+01	0.2166+01
0.3000+00	0.1064+01	0.1046+01	0.1018+01	0.2035+01
0.3200+00	0.1074+01	0.1052+01	0.1020+01	0.1922+01
0.3400+00	0.1083+01	0.1059+01	0.1023+01	0.1823+01
0.3600+00	0.1094+01	0.1066+01	0.1026+01	0.1736+01
0.3800+00	0.1105+01	0.1074+01	0.1029+01	0.1659+01
0.4000+00	0.1117+01	0.1082+01	0.1032+01	0.1590+01
0.4200+00	0.1129+01	0.1091+01	0.1035+01	0.1529+01
0.4400+00	0.1142+01	0.1100+01	0.1039+01	0.1474+01
0.4600+00	0.1156+01	0.1109+01	0.1042+01	0.1425+01
0.4800+00	0.1171+01	0.1119+01	0.1046+01	0.1380+01
0.5000+00	0.1186+01	0.1130+01	0.1050+01	0.1340+01
0.5200+00	0.1202+01	0.1141+01	0.1054+01	0.1303+01
0.5400+00	0.1219+01	0.1152+01	0.1058+01	0.1270+01
0.5600+00	0.1237+01	0.1164+01	0.1063+01	0.1240+01
0.5800+00	0.1256+01	0.1177+01	0.1067+01	0.1213+01
0.6000+00	0.1276+01	0.1190+01	0.1072+01	0.1188+01

Continued

Table A.1—*Continued*

M	$\frac{p_o}{p}$	$\frac{\rho_o}{\rho}$	$\frac{T_o}{T}$	$\frac{A}{A^*}$
0.6200+00	0.1296+01	0.1203+01	0.1077+01	0.1166+01
0.6400+00	0.1317+01	0.1218+01	0.1082+01	0.1145+01
0.6600+00	0.1340+01	0.1232+01	0.1087+01	0.1127+01
0.6800+00	0.1363+01	0.1247+01	0.1092+01	0.1110+01
0.7000+00	0.1387+01	0.1263+01	0.1098+01	0.1094+01
0.7200+00	0.1412+01	0.1280+01	0.1104+01	0.1081+01
0.7400+00	0.1439+01	0.1297+01	0.1110+01	0.1068+01
0.7600+00	0.1466+01	0.1314+01	0.1116+01	0.1057+01
0.7800+00	0.1495+01	0.1333+01	0.1122+01	0.1047+01
0.8000+00	0.1524+01	0.1351+01	0.1128+01	0.1038+01
0.8200+00	0.1555+01	0.1371+01	0.1134+01	0.1030+01
0.8400+00	0.1587+01	0.1391+01	0.1141+01	0.1024+01
0.8600+00	0.1621+01	0.1412+01	0.1148+01	0.1018+01
0.8800+00	0.1655+01	0.1433+01	0.1155+01	0.1013+01
0.9000+00	0.1691+01	0.1456+01	0.1162+01	0.1009+01
0.9200+00	0.1729+01	0.1478+01	0.1169+01	0.1006+01
0.9400+00	0.1767+01	0.1502+01	0.1177+01	0.1003+01
0.9600+00	0.1808+01	0.1526+01	0.1184+01	0.1001+01
0.9800+00	0.1850+01	0.1552+01	0.1192+01	0.1000+01
0.1000+01	0.1893+01	0.1577+01	0.1200+01	0.1000+01
0.1020+01	0.1938+01	0.1604+01	0.1208+01	0.1000+01
0.1040+01	0.1985+01	0.1632+01	0.1216+01	0.1001+01
0.1060+01	0.2033+01	0.1660+01	0.1225+01	0.1003+01
0.1080+01	0.2083+01	0.1689+01	0.1233+01	0.1005+01
0.1100+01	0.2135+01	0.1719+01	0.1242+01	0.1008+01
0.1120+01	0.2189+01	0.1750+01	0.1251+01	0.1011+01
0.1140+01	0.2245+01	0.1782+01	0.1260+01	0.1015+01
0.1160+01	0.2303+01	0.1814+01	0.1269+01	0.1020+01
0.1180+01	0.2363+01	0.1848+01	0.1278+01	0.1025+01
0.1200+01	0.2425+01	0.1883+01	0.1288+01	0.1030+01
0.1220+01	0.2489+01	0.1918+01	0.1298+01	0.1037+01
0.1240+01	0.2556+01	0.1955+01	0.1308+01	0.1043+01
0.1260+01	0.2625+01	0.1992+01	0.1318+01	0.1050+01
0.1280+01	0.2697+01	0.2031+01	0.1328+01	0.1058+01
0.1300+01	0.2771+01	0.2071+01	0.1338+01	0.1066+01
0.1320+01	0.2847+01	0.2112+01	0.1348+01	0.1075+01
0.1340+01	0.2927+01	0.2153+01	0.1359+01	0.1084+01
0.1360+01	0.3009+01	0.2197+01	0.1370+01	0.1094+01
0.1380+01	0.3094+01	0.2241+01	0.1381+01	0.1104+01
0.1400+01	0.3182+01	0.2286+01	0.1392+01	0.1115+01
0.1420+01	0.3273+01	0.2333+01	0.1403+01	0.1126+01
0.1440+01	0.3368+01	0.2381+01	0.1415+01	0.1138+01
0.1460+01	0.3465+01	0.2430+01	0.1426+01	0.1150+01
0.1480+01	0.3566+01	0.2480+01	0.1438+01	0.1163+01
0.1500+01	0.3671+01	0.2532+01	0.1450+01	0.1176+01
0.1520+01	0.3779+01	0.2585+01	0.1462+01	0.1190+01
0.1540+01	0.3891+01	0.2639+01	0.1474+01	0.1204+01
0.1560+01	0.4007+01	0.2695+01	0.1487+01	0.1219+01
0.1580+01	0.4127+01	0.2752+01	0.1499+01	0.1234+01
0.1600+01	0.4250+01	0.2811+01	0.1512+01	0.1250+01
0.1620+01	0.4378+01	0.2871+01	0.1525+01	0.1267+01
0.1640+01	0.4511+01	0.2933+01	0.1538+01	0.1284+01
0.1660+01	0.4648+01	0.2996+01	0.1551+01	0.1301+01
0.1680+01	0.4790+01	0.3061+01	0.1564+01	0.1319+01
0.1700+01	0.4936+01	0.3128+01	0.1578+01	0.1338+01
0.1720+01	0.5087+01	0.3196+01	0.1592+01	0.1357+01
0.1740+01	0.5244+01	0.3266+01	0.1606+01	0.1376+01
0.1760+01	0.5406+01	0.3338+01	0.1620+01	0.1397+01
0.1780+01	0.5573+01	0.3411+01	0.1634+01	0.1418+01
0.1800+01	0.5746+01	0.3487+01	0.1648+01	0.1439+01
0.1820+01	0.5924+01	0.3564+01	0.1662+01	0.1461+01
0.1840+01	0.6109+01	0.3643+01	0.1677+01	0.1484+01
0.1860+01	0.6300+01	0.3723+01	0.1692+01	0.1507+01
0.1880+01	0.6497+01	0.3806+01	0.1707+01	0.1531+01
0.1900+01	0.6701+01	0.3891+01	0.1722+01	0.1555+01
0.1920+01	0.6911+01	0.3978+01	0.1737+01	0.1580+01
0.1940+01	0.7128+01	0.4067+01	0.1753+01	0.1606+01
0.1960+01	0.7353+01	0.4158+01	0.1768+01	0.1633+01
0.1980+01	0.7585+01	0.4251+01	0.1784+01	0.1660+01
0.2000+01	0.7824+01	0.4347+01	0.1800+01	0.1687+01
0.2050+01	0.8458+01	0.4596+01	0.1840+01	0.1760+01
0.2100+01	0.9145+01	0.4859+01	0.1882+01	0.1837+01
0.2150+01	0.9888+01	0.5138+01	0.1924+01	0.1919+01
0.2200+01	0.1069+02	0.5433+01	0.1968+01	0.2005+01
0.2250+01	0.1156+02	0.5746+01	0.2012+01	0.2096+01
0.2300+01	0.1250+02	0.6076+01	0.2058+01	0.2193+01
0.2350+01	0.1352+02	0.6425+01	0.2104+01	0.2295+01
0.2400+01	0.1462+02	0.6794+01	0.2152+01	0.2403+01
0.2450+01	0.1581+02	0.7183+01	0.2200+01	0.2517+01
0.2500+01	0.1709+02	0.7594+01	0.2250+01	0.2637+01
0.2550+01	0.1847+02	0.8027+01	0.2300+01	0.2763+01
0.2600+01	0.1995+02	0.8484+01	0.2352+01	0.2896+01
0.2650+01	0.2156+02	0.8965+01	0.2404+01	0.3036+01
0.2700+01	0.2328+02	0.9472+01	0.2458+01	0.3183+01
0.2750+01	0.2514+02	0.1001+02	0.2512+01	0.3338+01
0.2800+01	0.2714+02	0.1057+02	0.2568+01	0.3500+01
0.2850+01	0.2929+02	0.1116+02	0.2624+01	0.3671+01
0.2900+01	0.3159+02	0.1178+02	0.2682+01	0.3850+01
0.2950+01	0.3407+02	0.1243+02	0.2740+01	0.4038+01
0.3000+01	0.3673+02	0.1312+02	0.2800+01	0.4235+01
0.3050+01	0.3959+02	0.1384+02	0.2860+01	0.4441+01
0.3100+01	0.4265+02	0.1459+02	0.2922+01	0.4657+01
0.3150+01	0.4593+02	0.1539+02	0.2984+01	0.4884+01
0.3200+01	0.4944+02	0.1622+02	0.3048+01	0.5121+01
0.3250+01	0.5320+02	0.1709+02	0.3112+01	0.5369+01
0.3300+01	0.5722+02	0.1800+02	0.3178+01	0.5629+01
0.3350+01	0.6152+02	0.1896+02	0.3244+01	0.5900+01
0.3400+01	0.6612+02	0.1996+02	0.3312+01	0.6184+01
0.3450+01	0.7103+02	0.2101+02	0.3380+01	0.6480+01
0.3500+01	0.7627+02	0.2211+02	0.3450+01	0.6790+01

Table A.1—*Continued*

M	$\frac{p_o}{p}$	$\frac{\rho_o}{\rho}$	$\frac{T_o}{T}$	$\frac{A}{A^*}$
0.3550+01	0.8187+02	0.2325+02	0.3520+01	0.7113+01
0.3600+01	0.8784+02	0.2445+02	0.3592+01	0.7450+01
0.3650+01	0.9420+02	0.2571+02	0.3664+01	0.7802+01
0.3700+01	0.1010+03	0.2701+02	0.3738+01	0.8169+01
0.3750+01	0.1082+03	0.2838+02	0.3812+01	0.8552+01
0.3800+01	0.1159+03	0.2981+02	0.3888+01	0.8951+01
0.3850+01	0.1241+03	0.3129+02	0.3964+01	0.9366+01
0.3900+01	0.1328+03	0.3285+02	0.4042+01	0.9799+01
0.3950+01	0.1420+03	0.3446+02	0.4120+01	0.1025+02
0.4000+01	0.1518+03	0.3615+02	0.4200+01	0.1072+02
0.4050+01	0.1623+03	0.3791+02	0.4280+01	0.1121+02
0.4100+01	0.1733+03	0.3974+02	0.4362+01	0.1171+02
0.4150+01	0.1851+03	0.4164+02	0.4444+01	0.1224+02
0.4200+01	0.1975+03	0.4363+02	0.4528+01	0.1279+02
0.4250+01	0.2108+03	0.4569+02	0.4612+01	0.1336+02
0.4300+01	0.2247+03	0.4784+02	0.4698+01	0.1395+02
0.4350+01	0.2396+03	0.5007+02	0.4784+01	0.1457+02
0.4400+01	0.2553+03	0.5239+02	0.4872+01	0.1521+02
0.4450+01	0.2719+03	0.5480+02	0.4960+01	0.1587+02
0.4500+01	0.2894+03	0.5731+02	0.5050+01	0.1656+02
0.4550+01	0.3080+03	0.5991+02	0.5140+01	0.1728+02
0.4600+01	0.3276+03	0.6261+02	0.5232+01	0.1802+02
0.4650+01	0.3483+03	0.6542+02	0.5324+01	0.1879+02
0.4700+01	0.3702+03	0.6833+02	0.5418+01	0.1958+02
0.4750+01	0.3933+03	0.7135+02	0.5512+01	0.2041+02
0.4800+01	0.4177+03	0.7448+02	0.5608+01	0.2126+02
0.4850+01	0.4434+03	0.7772+02	0.5704+01	0.2215+02
0.4900+01	0.4705+03	0.8109+02	0.5802+01	0.2307+02
0.4950+01	0.4990+03	0.8457+02	0.5900+01	0.2402+02
0.5000+01	0.5291+03	0.8818+02	0.6000+01	0.2500+02
0.5100+01	0.5941+03	0.9579+02	0.6202+01	0.2707+02
0.5200+01	0.6661+03	0.1039+03	0.6408+01	0.2928+02
0.5300+01	0.7457+03	0.1127+03	0.6618+01	0.3165+02
0.5400+01	0.8335+03	0.1220+03	0.6832+01	0.3417+02
0.5500+01	0.9304+03	0.1320+03	0.7050+01	0.3687+02
0.5600+01	0.1037+04	0.1426+03	0.7272+01	0.3974+02
0.5700+01	0.1154+04	0.1539+03	0.7498+01	0.4280+02
0.5800+01	0.1283+04	0.1660+03	0.7728+01	0.4605+02
0.5900+01	0.1424+04	0.1789+03	0.7962+01	0.4951+02
0.6000+01	0.1579+04	0.1925+03	0.8200+01	0.5318+02
0.6100+01	0.1748+04	0.2071+03	0.8442+01	0.5708+02
0.6200+01	0.1933+04	0.2225+03	0.8688+01	0.6121+02
0.6300+01	0.2135+04	0.2388+03	0.8938+01	0.6559+02
0.6400+01	0.2355+04	0.2562+03	0.9192+01	0.7023+02
0.6500+01	0.2594+04	0.2745+03	0.9450+01	0.7513+02
0.6600+01	0.2855+04	0.2939+03	0.9712+01	0.8032+02
0.6700+01	0.3138+04	0.3145+03	0.9978+01	0.8580+02
0.6800+01	0.3445+04	0.3362+03	0.1025+02	0.9159+02
0.6900+01	0.3779+04	0.3591+03	0.1052+02	0.9770+02
0.7000+01	0.4140+04	0.3833+03	0.1080+02	0.1041+03
0.7100+01	0.4531+04	0.4088+03	0.1108+02	0.1109+03
0.7200+01	0.4953+04	0.4357+03	0.1137+02	0.1181+03
0.7300+01	0.5410+04	0.4640+03	0.1166+02	0.1256+03
0.7400+01	0.5903+04	0.4939+03	0.1195+02	0.1335+03
0.7500+01	0.6434+04	0.5252+03	0.1225+02	0.1418+03
0.7600+01	0.7006+04	0.5582+03	0.1255+02	0.1506+03
0.7700+01	0.7623+04	0.5928+03	0.1286+02	0.1598+03
0.7800+01	0.8285+04	0.6292+03	0.1317+02	0.1694+03
0.7900+01	0.8998+04	0.6674+03	0.1348+02	0.1795+03
0.8000+01	0.9763+04	0.7075+03	0.1380+02	0.1901+03
0.9000+01	0.2110+05	0.1227+04	0.1720+02	0.3272+03
0.1000+02	0.4244+05	0.2021+04	0.2100+02	0.5359+03
0.1100+02	0.8033+05	0.3188+04	0.2520+02	0.8419+03
0.1200+02	0.1445+06	0.4848+04	0.2980+02	0.1276+04
0.1300+02	0.2486+06	0.7144+04	0.3480+02	0.1876+04
0.1400+02	0.4119+06	0.1025+05	0.4020+02	0.2685+04
0.1500+02	0.6602+06	0.1435+05	0.4600+02	0.3755+04
0.1600+02	0.1028+07	0.1969+05	0.5220+02	0.5145+04
0.1700+02	0.1559+07	0.2651+05	0.5880+02	0.6921+04
0.1800+02	0.2311+07	0.3512+05	0.6580+02	0.9159+04
0.1900+02	0.3356+07	0.4584+05	0.7320+02	0.1195+05
0.2000+02	0.4783+07	0.5905+05	0.8100+02	0.1538+05
0.2200+02	0.9251+07	0.9459+05	0.9780+02	0.2461+05
0.2400+02	0.1691+08	0.1456+06	0.1162+03	0.3783+05
0.2600+02	0.2949+08	0.2165+06	0.1362+03	0.5624+05
0.2800+02	0.4936+08	0.3128+06	0.1578+03	0.8121+05
0.3000+02	0.7978+08	0.4408+06	0.1810+03	0.1144+06
0.3200+02	0.1250+09	0.6076+06	0.2058+03	0.1576+06
0.3400+02	0.1908+09	0.8216+06	0.2322+03	0.2131+06
0.3600+02	0.2842+09	0.1092+07	0.2602+03	0.2832+06
0.3800+02	0.4143+09	0.1430+07	0.2898+03	0.3707+06
0.4000+02	0.5926+09	0.1846+07	0.3210+03	0.4785+06
0.4200+02	0.8330+09	0.2354+07	0.3538+03	0.6102+06
0.4400+02	0.1153+10	0.2969+07	0.3882+03	0.7694+06
0.4600+02	0.1572+10	0.3706+07	0.4242+03	0.9603+06
0.4800+02	0.2116+10	0.4583+07	0.4618+03	0.1187+07
0.5000+02	0.2815+10	0.5618+07	0.5010+03	0.1455+07